RSC Advances

PAPER

View Article Online
View Journal | View Issue

Cite this: *RSC Adv.*, 2017, **7**, 52755

Insights into TiO_2 polymorphs: highly selective synthesis, phase transition, and their polymorph-dependent properties

Maolin Zhang,[ac] Tiedan Chen[b] and Yunjian Wang *[b]

Despite the enormous efforts devoted to the research of titanium dioxide (TiO_2), controlling TiO_2 polymorphism, size and morphology still represents an interesting challenge since its stabilities, transitions and properties vary with them. Herein, we report a novel selective-synthesis of high purity anatase (A), rutile (R) and brookite (B) phase TiO_2 from solution under mild hydrothermal conditions. By adjusting the concentrations of chloroacetic acid, urea and sodium hydroxide, A-TiO_2 nanocrystals, R-TiO_2 nanorods and B-TiO_2 hollow spheres and nanorods can be easily produced as investigated by XRD and TEM characterisation. Based on time-varied experiments, two distinct phase transitions were observed under different hydrothermal conditions, namely the initially formed A-TiO_2 nanocrystals would transform into R-TiO_2 nanorods with augmented crystalline size under acidic conditions while they transformed into B-TiO_2 hollow spheres under basic conditions. Moreover, polymorph formation and transition mechanism were explored in detail based on systematic investigation into the effects of synthetic parameters on the products. Finally, the spectra and photocatalytic properties of the three polymorphs were investigated and discussed. The synthetic approach reported here allows for full control over polymorph selection in TiO_2 crystallization and provides new insights in this area.

Received 18th October 2017
Accepted 9th November 2017

DOI: 10.1039/c7ra11515f

rsc.li/rsc-advances

Introduction

Over the past decades, TiO_2 nanomaterials have continued to be the most popular photocatalysts for their high chemical activity and stability, environmental benignity and low cost.[1–5] It is known that the properties of TiO_2 nanomaterials are a function of particle size, morphology, and crystal structure. Therefore, enormous interest has been devoted to their size, morphology, and crystal structure-controlled synthesis, which has resulted in a rich database for their synthetic methodology and size or structure-dependent properties.[6–11] TiO_2 occurs in nature as the well-known minerals anatase, rutile and brookite. In fact, the crystal structures of anatase, rutile and brookite are all built from distorted TiO_6 polyhedral units, but in different connection ways.[12,13] It is widely recorded that anatase and brookite are metastable phases, and both would transform into the thermodynamically stable rutile phase under pressure, heat or other conditions.[14–16] Nevertheless, synthesis of TiO_2 by common solution methods often results in the crystallization of anatase with the size ranging from 6–30 nm.[17–20] Rutile is stable at a large size, and common synthesis usually yields the rod-like products with the size above 35 nm, which is disadvantageous to photocatalytic activity. As for brookite, it remains to be the least prepared and studied phase, mainly owing to the difficulties encountered in obtaining its pure phase.[21–24] Perhaps for these reasons, most early researches on photocatalysis are focused on anatase, and thus generally conclude that anatase is the best candidate in photocatalytic applications.[25–27] Last several years, accompanied by the progress in the controlled synthesis of TiO_2 nanoparticles are some new findings and cognition on the photocatalytic activity of rutile and brookite TiO_2. For instance, Lin *et al.* reports that brookite TiO_2 nanosheet shows unexpected excellent photocatalytic performance due to specific crystal surface exposure.[28] Alike, it is also reported in some cases the rutile phase exhibits higher photocatalytic activity than its anatase counterpart.[29,30] This demonstrates that besides the well-known structure-dependent photocatalytic property, the size, as well as shape is equally important for photocatalytic activity. Therefore, progress in the selective synthesis of TiO_2 nanocrystallites allows for further understanding their polymorph-dependent properties and potential applications, and will continue to be interesting themes in TiO_2 research.

Many synthetic methods have been used to preparing TiO_2 nanocrystals, among which hydrothermal synthesis is proved to be the most effective approach to obtaining TiO_2 polymorphs by changing synthetic parameters, such as pH, reactant

[a]*Department of Materials and Chemical Engineering, Bengbu University, Bengbu 233030, P. R. China*

[b]*Key Laboratory of Energetic Materials of Anhui Province, College of Chemistry and Materials Science, Huaibei Normal University, 100 Dongshan Road, Huaibei 235000, P. R. China. E-mail: wangyunjianmail@163.com*

[c]*Information College, Huaibei Normal University, Huaibei 235000, P. R. China*

concentration, and the mineralizer used. Herein, we provide a novel highly selective hydrothermal preparation of anatase, rutile and especially brookite TiO_2 polymorphs under mild hydrothermal conditions. With titanyl sulfate as titanium source, anatase nanoparticles, rutile nanorods and brookite nanorods and hollow spheres were successfully synthesized by adjusting the addition of chloroacetic acid, urea and sodium hydroxide. The impacts of synthetic parameters on the phase formation and stability were discussed. The as-prepared pure phase powders were characterized by combined means of XRD, TEM, FT-IR and UV-vis spectroscopies. Moreover, the polymorph-dependent photocatalytic activities were evaluated by the degradation of methyl orange under UV illumination.

Experimental

Materials

Titanium oxysulfate ($TiOSO_4 \cdot xH_2SO_4 \cdot 8H_2O$) was purchased from Aladdin Chemical Reagent Corp. AR chloroacetic acid, urea and sodium hydroxide were purchased from Sinopharm Chemical Reagent Co., Ltd and used as received without any further purification. Deionized water was used for the preparation of the solution and synthesis in all the experiments.

Synthesis of TiO_2 polymorphs

All TiO_2 samples were prepared by a typical hydrothermal approach according to the following procedures.

Synthesis of A-TiO_2. 2.63 g titanium sulfate was dispersed in 50 mL water under constant stirring and then 15 g urea and giving amount of chloroacetic acid were added into the above solution and was stirred for 2 h, and then transferred into a 100 mL Teflon-lined stainless steel autoclave that was allowed to react at 200 °C for 9 h. Finally, the products were centrifuged and washed with deionized water several times, and then dried at 80 °C for 12 h.

Synthesis of R-TiO_2. 2.63 g titanium sulfate was dispersed in 50 mL water under constant stirring and then 5 g chloroacetic acid, 4.25 g NaOH were added into the above solution and was stirred for 2 h, and then transferred into a 100 mL Teflon-lined stainless steel autoclave that was allowed to react at 200 °C for 36 h. As we known, it is easy to obtain anatase in the hydrothermal synthesis. Thus, A-TiO_2 formed in the synthesis of both R-TiO_2 and B-TiO_2 processes as the synthetic parameters changed.

Synthesis of B-TiO_2. 2.63 g titanium sulfate was dispersed in 50 mL water under constant stirring and then 5 g chloroacetic acid, 15 g urea and 2.12 g NaOH were added into the above solution and was stirred for 2 h until the solution became a translucent yellow, and then transferred into a 100 mL Teflon-lined stainless steel autoclave that was allowed to react at 200 °C for 9 h. The pH of the solution was adjusted by changing the addition of NaOH.

Characterization

XRD was performed on a Bruker D8 Advance X-ray powder diffractometer equipped with Cu Kα radiation ($\lambda = 1.5406$ Å) at 40 kV and 40 mA. Morphologies of the samples were examined by using a transmission electron microscope (TEM TecnaiTF20) with an acceleration voltage of 200 kV. Infrared spectra of the samples were measured on a Perkin-Elmer IR spectrophotometer at a resolution of 4 cm^{-1} by KBr pellet technique. UV-vis diffuse reflectance spectra were collected using a TU-1901 UV-vis spectrophotometer (Beijing Purkinje General Instrument Co., Ltd.) equipped with an integrating sphere attachment. The photocatalytic activities were evaluated by the degradation of methyl orange (MO) solution at room temperature. All experiments were carried out as follows: 80 mg of the photocatalyst was dispersed in 80 mL of 10 ppm MO aqueous solution in a quartz tube with 4.6 cm diameter and 17 cm length. Prior to illumination, the suspensions were magnetically stirred in the dark for 2 h to ensure the establishment of absorption/desorption equilibrium of MO on the sample surfaces. Subsequently, the suspension was irradiated around by four UV lamps with wavelength centred at 254 nm (Philips, TUV 4W/G4 T5).

Results and discussion

A-TiO_2, R-TiO_2 and especially B-TiO_2 were successfully prepared by using chloroacetic acid as surface capping agent and adjusting the urea and NaOH concentration under mild hydrothermal condition. The detailed results and the effect of synthetic parameter were discussed as follows.

A-TiO_2 nanocrystals made with urea

Fig. 1 shows the XRD patterns of the samples prepared with urea under giving chloroacetic acid concentrations. It is seen that the powders prepared under different chloroacetic acid concentrations are well crystallized anatase. Using Scherrer equation, the average crystalline sizes for the samples were calculated to be 12.5, 12.1, 13.9, and 9.2 nm, respectively. Further TEM analysis found that the morphologies of the A-

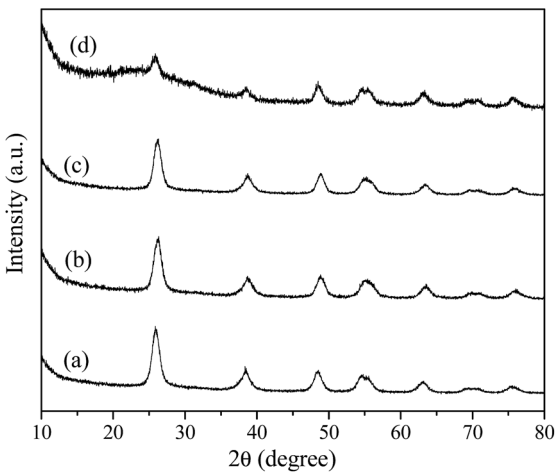

Fig. 1 XRD patterns of the samples prepared using urea under varied chloroacetic acid concentrations (a) 0, (b) 0.25, (c) 0.5 and (d) 0.75 mol L^{-1}.

TiO_2 were tunable by changing the chloroacetic acid concentrations. As shown in Fig. 2a and b, uniform nanoparticles with the particle size about 30 nm were obtained in the absence of chloroacetic acid. Micro spheres self-assembled by nanoparticles were obtained under 0.5 M chloroacetic acid condition, as displayed in Fig. 2c and d. It should be noted that the product became the mixture of anatase and amorphous TiO_2 as the chloroacetic acid concentrations increased up to 0.75 M, indicating that amorphous products can be easily formed in acidic conditions.

R-TiO_2 nanocrystals made with NaOH

As mentioned above, only A-TiO_2 was obtained by employing urea with or without the adding of chloroacetic acid. In order to control the polymorph crystallization, NaOH instead of urea were used. Previous work reports rutile is thermodynamically stable phase and in usual anatase can convent into rutile under various conditions, including milling, laser or heat treatment.[31–33] To investigate the polymorph formation and transition process, a series of time-resolved experiments with fixed NaOH (2 M), chloroacetic acid (0.75 M) concentration and reaction temperature (200 °C) were carried out. Fig. 3 shows the corresponding XRD patterns of powders synthesized for different periods of hydrothermal time. It is noted that the product was exclusively anatase nanocrystals with 5 nm size (Fig. 4a) when reaction time was as short as 1 h. Prolonging the reaction time to 3 h, the product was a mixed phase of anatase and rutile with apparent changes in particle morphology (Fig. 4b). Further prolonging the reaction time, these anatase nanoparticles gradually disappeared while the rutile increased. In the time range from 3 to 18 h, the mixture of anatase nanoparticles and rutile nanorods was obtained (Fig. 4c). Pure-phase rutile nanorods with diameters of 20 nm and lengths of up to 150 nm were obtained after 36 h reactions (Fig. 4d). These observations strongly indicated that the formation of rutile nanorods was originated from the direct transformation of the anatase precursor. This observation is interesting and important since anatase to rutile transition requires high temperature. As previous literatures revealed, the preferential growth along [001] direction is the reason why rutile frequently crystallizes in rod like and rarely crystallizes in rounded shapes. This preferential growth in solution is arising from the unique crystal structure of rutile. In this work, rutile was prepared in basic environment (2 M NaOH), distinction from previous reports, in which pure rutile can only be formed under highly acidic conditions, irrespective of the titanium type and concentration.[34]

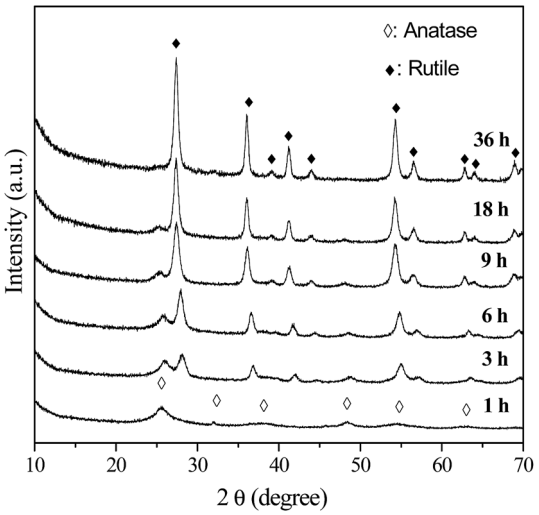

Fig. 3 XRD patterns of the samples prepared in 2 M NaOH, 0.75 M chloroacetic acid for different periods of hydrothermal time.

B-TiO_2 nanocrystals made with urea and NaOH

As one of the most attractive TiO_2 polymorphs, brookite with several morphologies has been reported in the literature. For

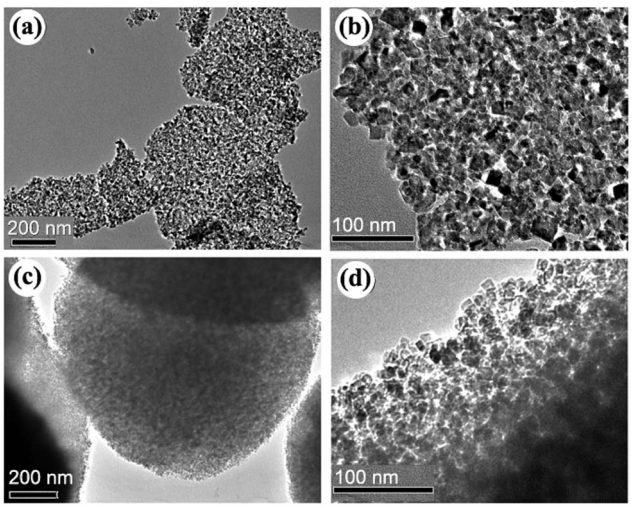

Fig. 2 TEM images of the samples prepared in the absence chloroacetic acid (a, b) and (c, d) 0.5 M chloroacetic acid.

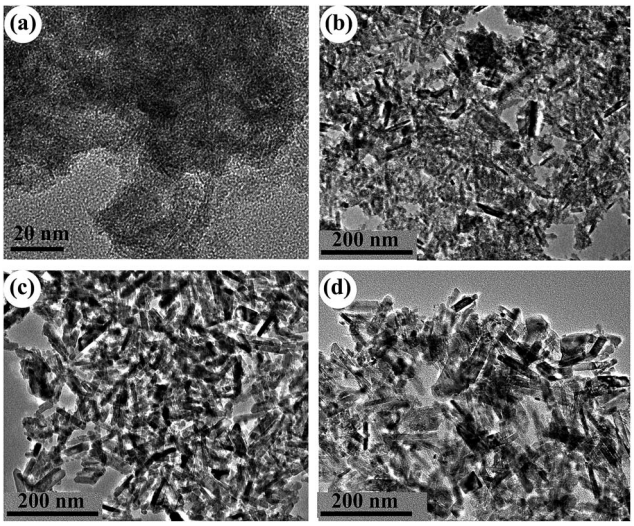

Fig. 4 TEM images of the samples prepared in 2 M NaOH, 0.75 M chloroacetic acid for different periods of hydrothermal time: (a) 1 h; (b) 3 h; (c) 18 h and (d) 36 h.

example, Bahnemann *et al.*, prepared phase-pure brookite nanorods by the thermal hydrolysis of commercially available aqueous solutions of titanium bis(ammonium lactate) dihydroxide.[35] Herein, we initially adopted a simple formation of phase-pure brookite under hydrothermal condition by employing common reagents chloroacetic acid, urea, and NaOH. Fig. 5 shows XRD patterns of the samples prepared at 200 °C for 9 h with varied pH values adjusted by changing NaOH addition. When the pH value was 2, the product was a mixture of anatase and amorphous TiO_2, which is in good agreement with previous result (Fig. 1d). According to early literatures, phase purity of brookite can be estimated by the intensity ratio of diffraction peaks, $I_{121}^{brookite}/(I_{120}^{brookite} + I_{101}^{anatase})$.[13,36] Adjusting the pH value to 3 by increasing the NaOH amount, the obtained product was high pure brookite self-assembled hollow spheres (Fig. 6a), for the second diffraction from (121) was almost equal to the strongest diffraction from brookite (120), indicating high purity of the brookite. The product was still pure brookite as the pH value was increased to 5 while the morphology became nanorods (Fig. 6b). In neutral condition of pH = 7, the product became pure phase anatase. Interesting, anatase with trace brookite was obtained when increase pH up to 9. Further increase pH value to 13 leads to the conformation of brookite (79%) and a small amount of anatase (21%). These observations demonstrated that brookite can be prepared under acidic or alkaline conditions. It is important since early work concluded that brookite usually crystallize in strong alkaline solution.[28,37] Besides, it should be mentioned that the as-prepared brookite was characterized by its purity since many of the previously claimed pure brookite powders show $I_{121}^{brookite}/I_{120}^{brookite}$ ratios lower than 0.9, indicating coexistence of anatase phase.

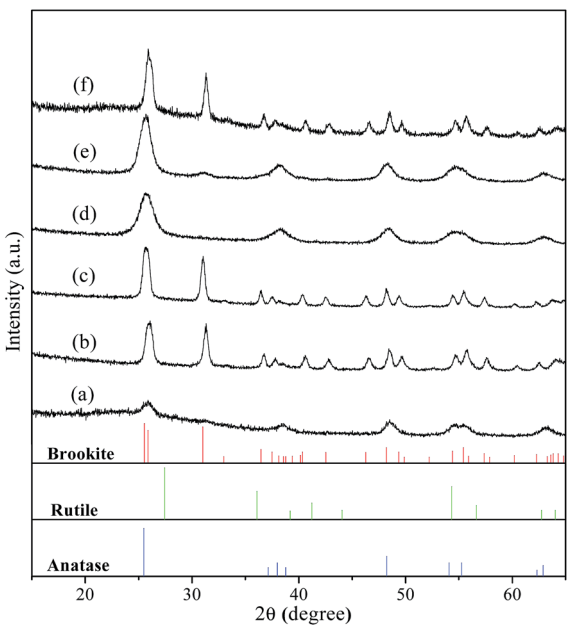

Fig. 5 XRD patterns of the samples prepared in 0.75 M chloroacetic acid at 200 °C for 9 h with varied pH values adjusted by changing NaOH addition: (a) pH = 2; (b) pH = 3; (c) pH = 5; (d) pH = 7; (e) pH = 9; and (f) pH = 13. Vertical bars in bottom layers denote the standard data of anatase (JCPDS no. 71-1167), rutile (JCPDS no. 21-1276), and brookite (JCPDS no. 29-1360), respectively.

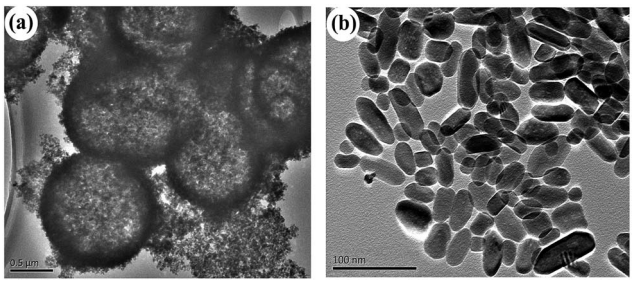

Fig. 6 TEM images of the pure phase brookite samples prepared under (a) pH = 3 (S2) and (b) pH = 5 (S3).

To explore the role of urea on the brookite crystallization, another set of experiments were carried out with varying urea concentrations by setting NaOH concentration at 2 M and chloroacetic acid concentration at 0.75 M, respectively. As seen from Fig. 7, rutile with a small amount of anatase was obtained in the absence of urea. Meanwhile, brookite can be formed in a wide range of urea concentration from 1.67 to 5 M. As proved above, anatase was able to transform to rutile by expanding hydrothermal reaction time. To understand the formation process of brookite, a series of time-resolved experiments with other synthetic parameters fixed were carried out, as shown in Fig. 8. It is found that the product was a mixture of amorphous, anatase and brookite at the initial stage of the reaction (1 h). Amorphous is a common product in the low temperature synthesis of TiO_2, which can transform into anatase, rutile or brookite depending on solution environment. Increasing of reaction time resulted in the steadily decreasing of anatase content and finally led to pure brookite when the reaction time to 9 h. From this result and above, it is easy to conclude that both amorphous and anatase were able to transform into rutile in the absence of urea (Fig. 3) while they transformed into brookite in urea solution (Fig. 8). Different from our result,

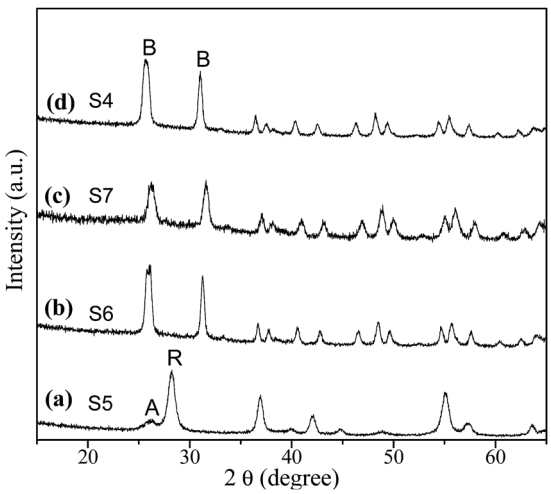

Fig. 7 XRD patterns of the samples prepared under different urea concentrations: (a) 0, (b) 1.67, (c) 3.35 and (d) 5 mol L^{-1}.

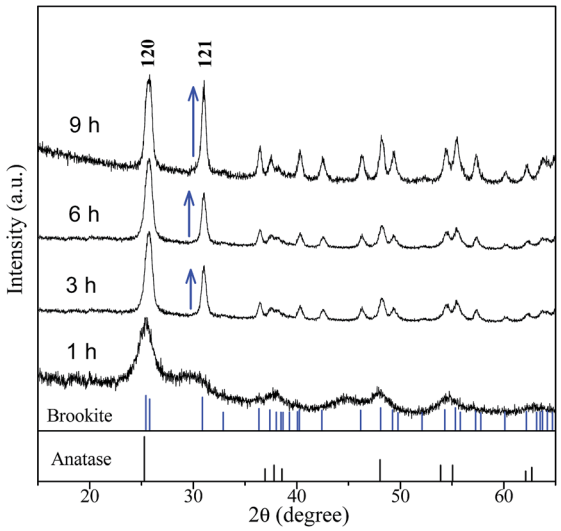

Fig. 8 XRD patterns of the samples prepared at 200 °C, pH = 3, at different reaction times.

Table 1 Experimental conditions and products in the hydrothermal preparation of TiO_2 polymorphs[a]

	Reagents concentrations (M)			Conditions	
	NaOH	Urea	Chloroacetic acid	Tem./time	Products
S1	0	5	1	200 °C/9 h	A
S2	1	5	1	200 °C/9 h	B
S3	2	5	1	200 °C/9 h	B
S4	3	5	1	200 °C/9 h	B + A (trace)
S5	2	0	1	200 °C/9 h	R + R (trace)
S6	2	1.7	1	200 °C/9 h	B
S7	2	3.4	1	200 °C/9 h	B
S8	0	5	0	200 °C/9 h	A
S9	0	5	0.25	200 °C/9 h	A
S10	0	5	0.5	200 °C/9 h	A
S11	2	0	1	200 °C/1 h	A
S12	2	0	1	200 °C/3 h	A + R
S13	2	0	1	200 °C/36 h	R

[a] $TiOSO_4$ concentration was 0.22 M and unchanged in all experiments.

most several literatures reports that rutile or brookite could be transformed from amorphous TiO_2 precursor rather than anatase under different hydrothermal condition.[38] As a matter of fact, the formation mechanism and phase transition of brookite is still controversial especially in solution. As we known, it is generally thought that TiO_2 polymorphs showed the size-dependent stability, controlled by surface energy. Anatase is the most stable at smaller sizes (below 11 nm) while rutile and brookite in bigger size.[39] Indeed, evident crystalline size increase and morphologies change were observed in both transitions, revealing that structural reorganization took place in these transitions. In this regard, anatase tends to crystalline into particles while rutile into rods, as we shown. Combined with the results above (Fig. 1, 5 and 6), we can easily conclude that chloroacetic acid, pH value and urea are essential factors for the crystallization of brookite. The crystallization of TiO_2 polymorphs is high sensitive to synthetic environment under hydrothermal condition. To illustrate the impact of synthetic parameters clearly, the synthetic conditions and phase constituents are summarized in Table 1.

The FT-IR spectrum is effective to detect the surface adsorbate, as shown in Fig. 9. It is noted that several absorptions were observed at wavelength of 3450, 1640, and 602 cm^{-1}, respectively. The appearances of absorption bands at 3450 and 1640 cm^{-1} suggest the existence of hydration water on the surface of the three samples. Another vibration at 602 cm^{-1} was the characteristic of the bending vibrations of Ti–O in TiO_6 octahedron, which shows no obvious difference among three samples. Fig. 10 shows the UV-vis spectra of the hydrothermal prepared different TiO_2 polymorphs. It is seen that optical absorption edges of the anatase, rutile, and brookite polymorphs were located at 410, 419, and 405 nm, respectively. According to plenty of literature work, anatase is an indirect transition semiconductor while rutile and brookite are direct-transition semiconductors.[37,40,41] According to the plots of $(F(R) \times h\nu)^n$ *vs.* energy ($h\nu$) in the insert of Fig. 10, the band gap E_g were determined to be 3.22, 3.0, and 3.23 eV for the anatase, rutile and brookite, respectively. The value of brookite obtained in the present work is the a little smaller than the reported value.[42]

The photocatalytic activity of the TiO_2 polymorphs was tested by the degradation of 10 ppm methyl orange solutions at natural pH values under UV light. Fig. 11 shows the degradation kinetics of MO over different TiO_2 polymorphs. Evidently, anatase shows the best photocatalytic activity with 90% degraded within 2 hours while in the presence of rutile, only 60% MO molecular was degraded in the same time. Brookite shows the worst photocatalytic activity among. There was little different in photocatalytic activity between brookite hollow spheres and nanorods. The photocatalytic activity order for three polymorphs obtained here is in agreement with most previous studies.[43–45] There are several literatures reporting that the photocatalytic activity of rutile TiO_2 is better than its anatase

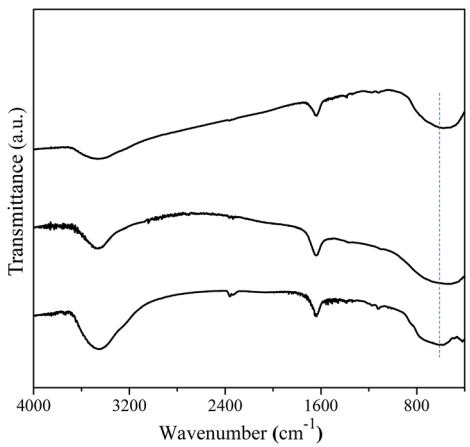

Fig. 9 FT-IR spectra of the as-prepared A-TiO_2 (S1), R-TiO_2 (S13) and B-TiO_2 (S6) samples.

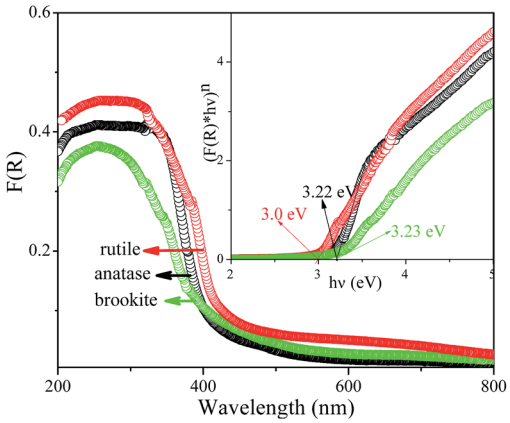

Fig. 10 UV-vis spectra of the as-prepared A-TiO_2 (S1), R-TiO_2 (S13) and B-TiO_2 (S6) samples.

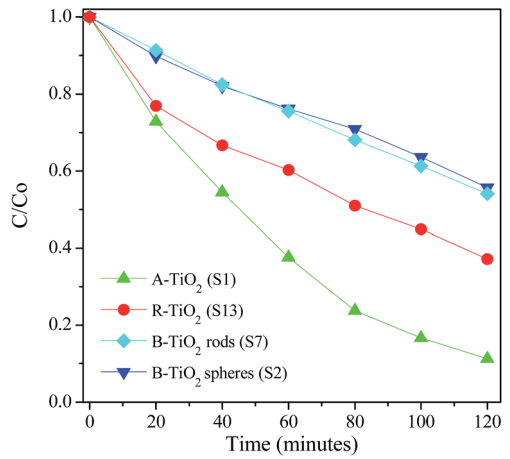

Fig. 11 Degradation kinetics of MO solutions over A-TiO_2 (S1), R-TiO_2 (S13) and B-TiO_2 nanorods (S6) and hollow spheres (S2) under UV irradiation.

counterpart.[46] It is well documented that the photocatalytic activity of TiO_2 is closely related to several factors, such as crystal structure, crystalline size, defect concentration, exposing crystal surface, *etc.*, all of which are determined by synthetic conditions. Therefore, it is understandable for the different order of photocatalytic properties among TiO_2 polymorphs reported in the literature. We believe that the unique crystal structure and crystallite shape of anatase are responsible for the excellent photocatalytic performance in our study.

Conclusions

In summary, we have demonstrated a facile method for the selective synthesis of A, R or B-type TiO_2 polymorph under hydrothermal condition. Anatase nanoparticles, rutile nanorods, and especially brookite hollow spheres and nanorods are successfully synthesized by adjusting the amount of chloroacetic acid, urea and NaOH. The use of chloroacetic acid and urea consistently yields anatase, and the morphology of the anatase particles can be controlled from dispersed nanocrystals to sphere-structured agglomerates by changing the chloroacetic acid concentration. The combined use of chloroacetic acid and NaOH leads to the formation of anatase, rutile and their mixtures by controlling the hydrothermal reaction time. It is found that rutile formed from anatase-to-rutile transition under hydrothermal condition. Nevertheless, the combined use of chloroacetic acid, urea and NaOH yields high pure brookite with the morphology from nanorods and self-assemble hollow spheres. Unlike rutile, brookite seems formed directly from the precursor rather than anatase, in agreement with previous discovery. Finally, the photocatalytic activity of three polymorphs of TiO_2 was compared. We believe that the method reported here provide new perspectives for the facile selective preparation of inorganic materials, especially for TiO_2 polymorphs, and thus allow for study on relevant structure-dependent properties.

Conflicts of interest

There are no conflicts to declare.

Acknowledgements

This work was financially supported by the Natural Science Foundation of Educational Committee of Anhui Province (No. KJ2014B08, KJ2017A386, KJ2017A841) and the Open Project of State Key Laboratory of Inorganic Synthesis and Preparative Chemistry, Jilin University (Grant Number: 2017-25).

Notes and references

1 X. B. Chen and S. M. Samuel, *Chem. Rev.*, 2007, **107**, 2891–2959.
2 H. Tong, S. X. Ouyang, Y. P. Bi, N. Umezawa, M. Oshikiri and J. H. Ye, *Adv. Mater.*, 2012, **24**, 229–251.
3 Y. Bai, I. Mora-Sero, F. De Angelis, J. Bisquert and P. Wang, *Chem. Rev.*, 2014, **114**, 10095–10130.
4 M. Cargnello, T. R. Gordon and C. B. Murray, *Chem. Rev.*, 2014, **114**, 9319–9345.
5 J. G. Yu, J. X. Low, W. Xiao, P. Zhou and M. Jaroniec, *J. Am. Chem. Soc.*, 2014, **136**, 8839–8842.
6 Y. S. Xu, H. F. Xu, L. P. Li, X. S. Huang and G. S. Li, *J. Mater. Chem. A*, 2015, **3**, 22361–22368.
7 G. L. Xiang, T. Y. Li, J. Zhuang and X. Wang, *Chem. Commun.*, 2010, **46**, 6801–6803.
8 G. Liu, H. G. Yang, J. Pan, Y. Q. Yang, G. Q. Lu and H. M. Cheng, *Chem. Rev.*, 2014, **114**, 9559–9612.
9 J. X. Low, B. Cheng and J. G. Yu, *Appl. Surf. Sci.*, 2017, **392**, 658–686.
10 S. W. Liu, J. G. Yu and M. Jaroniec, *J. Am. Chem. Soc.*, 2010, **132**, 11914–11916.
11 Y. Q. Yang, G. Liu, J. T. S. Irvine and H. M. Cheng, *Adv. Mater.*, 2016, **28**, 5850–5856.
12 W. B. Hu, L. P. Li, G. S. Li, Y. Liu and R. L. Withers, *Sci. Rep.*, 2014, **4**, 6582–6590.

13 J. G. Li, T. Ishigaki and X. D. Sun, *J. Phys. Chem. C*, 2007, **111**, 4969–4976.
14 K. Sabyrov, N. D. Burrows and R. L. Penn, *Chem. Mater.*, 2013, **25**, 1408–1415.
15 Q. Xu, J. Zhang, Z. C. Feng, Y. Ma, X. Wang and C. Li, *Chem.–Asian J.*, 2010, **5**, 2158–2161.
16 M. P. Finnegan, H. Z. Zhang and J. F. Banfield, *J. Phys. Chem. C*, 2007, **111**, 1962–1968.
17 K. Nakataa and A. Fujishima, *J. Photochem. Photobiol., C*, 2012, **13**, 169–189.
18 W. B. Hu, Y. L. Yu, H. Chen, K. Lau, V. Craig, F. Brink, R. L. Withers and Y. Liu, *Appl. Surf. Sci.*, 2015, **357**, 2022–2027.
19 X. Yu, Z. H. Zhao, J. Zhang, W. B. Guo, L. L. Li, H. Liu and Z. L. Wang, *CrystEngComm*, 2017, **19**, 129–136.
20 X. J. Zhang, G. Q. Zuo, X. Lu, C. Q. Tang, S. Cao and M. Yu, *J. Colloid Interface Sci.*, 2017, **490**, 774–782.
21 A. D. Paola, M. Bellardita and L. Palmisano, *Catalysts*, 2013, **3**, 36–73.
22 M. Bellarditaa, A. D. Paolaa, B. Megna and L. Palmisano, *Appl. Catal., B*, 2017, **201**, 150–158.
23 X. L. Che, L. P. Li, J. Zheng, G. S. Li and Q. Shi, *J. Chem. Thermodyn.*, 2016, **93**, 45–51.
24 J. L. Xu, S. F. Wu, J. P. Jin and T. Y. Peng, *Nanoscale*, 2016, **8**, 18771–18781.
25 M. Li, Y. Chen, W. Li, X. Li, H. Tian, X. Wei, Z. H. Ren and G. R. Han, *Small*, 2017, **13**, 1604115.
26 G. Liu, C. H. Sun, H. G. Yang, S. C. Smith, L. Z. Wang, G. Q. Lu and H. M. Cheng, *Chem. Commun.*, 2010, **46**, 755–757.
27 T. Luttrell, S. Halpegamage, J. Tao, A. Kramer, E. Sutter and M. Batzill, *Sci. Rep.*, 2014, **4**, 4043.
28 H. F. Lin, L. P. Li, M. L. Zhao, X. S. Huang, X. M. Chen, G. S. Li and R. C. Yu, *J. Am. Chem. Soc.*, 2012, **134**, 8328–8331.
29 B. Sun, G. W. Zhou, Y. Zhang, R. R. Liu and T. D. Li, *Chem. Eng. J.*, 2015, **264**, 125–133.
30 S. Yurdakal, G. Palmisano, V. Loddo, V. Augugliaro and L. Palmisano, *J. Am. Chem. Soc.*, 2008, **130**, 1568–1569.
31 G. C. Vásquez, M. A. Peche-Herrero, D. Maestre, A. Gianoncelli, J. Ramírez-Castellanos, A. Cremades, J. M. González-Calbet and J. Piqueras, *J. Phys. Chem. C*, 2015, **119**, 11965–11974.
32 E. Napolitano, G. Mulas, S. Enzo and F. Delogu, *Acta Mater.*, 2010, **58**, 3798–3804.
33 M. Rezaee, S. M. Mousavi Khoie and K. H. Liu, *CrystEngComm*, 2011, **13**, 5055–5061.
34 D. A. H. Hanaor and C. C. Sorrell, *J. Mater. Sci.*, 2011, **46**, 855–874.
35 T. A. Kandiel, L. Robben, A. Alkaimad and D. Bahnemann, *Photochem. Photobiol. Sci.*, 2013, **12**, 602–609.
36 H. Kominami, M. Kohno and Y. Kera, *J. Mater. Chem.*, 2000, **10**, 1151–1156.
37 W. B. Hu, L. P. Li, G. S. Li, C. L. Tang and L. Sun, *Cryst. Growth Des.*, 2009, **9**, 3676–3682.
38 H. B. Yin, Y. J. Wada, T. Kitamura, S. Kambe, S. Murasawa, H. Mori, T. Sakata and S. Yanagida, *J. Mater. Chem.*, 2001, **11**, 1694–1703.
39 M. A. Henderson, *Surf. Sci. Rep.*, 2011, **66**, 185–297.
40 S. D. Mo and W. Y. Ching, *Phys. Rev. B: Condens. Matter Mater. Phys.*, 1995, **51**, 13023.
41 A. Beltran, L. Gracia and J. Andres, *J. Phys. Chem. B*, 2006, **110**, 23417–23423.
42 M. Koelsch, S. Cassaignon, J. F. Guillemoles and J. P. Jolivet, *Thin Solid Films*, 2002, **403**, 312–319.
43 L. E. Oi, M. Y. Choo, H. V. Lee, H. C. Ong, S. B. A. Hamida and J. C. Juan, *RSC Adv.*, 2016, **6**, 108741–108754.
44 L. Liu, H. L. Liu, H. Zhao, J. M. Andino and Y. Li, *ACS Catal.*, 2012, **2**, 1817–1828.
45 A. Fujishima, X. Zhang and D. Tryk, *Surf. Sci. Rep.*, 2008, **63**, 515–582.
46 B. Sun, G. W. Zhou, Y. Zhang, R. R. Liu and T. D. Li, *Chem. Eng. J.*, 2015, **264**, 125–133.